Screening anti-inflammatory compounds in spinal cord injury using microarrays: Identification of therapies and potential mechanisms using a bioinformatics analysis.

Jonathan Z. Pan[1], Rebecka Jörnsten[2] and Ronald P. Hart[1]

[1]W.M Keck Center for Collaborative Neuroscience

[2]Department of Statistics

Rutgers, The State University of New Jersey

Piscataway, New Jersey 08854

DRAFT

Abstract

Inflammatory responses contribute to secondary tissue damage following spinal cord injury (SCI). A potent anti-inflammatory drug, methylprednisolone (MP) is the only currently accepted therapy for acute SCI. In order to search for novel mechanisms, we compared several anti-inflammatory compounds using our previously-described slice culture model of injury. Spinal cords were removed from drug pretreated rats, dissected into slices, and incubated with compounds or vehicle for 4 hrs. Using custom rat microarrays and quantitative real-time PCR (Q-RT-PCR), we studied gene expression profiles after treatment with MP, acetaminophen, indomethacin, NS398, combined IL-1ra (receptor antagonist) and soluble TNFR:Fc chimeric protein. Fresh and injured conditions without treatments were also included as controls. Multiple statistical analyses (principal components analysis [PCA], gene shaving; and K-medians/relative data depth [ReD]) were applied to the multi-dimensional data set and results were compared. Our analysis consistently showed a unique gene expression profile by NS398, the selective COX-2 inhibitor, in which the overall effect of these up-regulated genes could be associated with a proposed neuroprotective effect. In summary, using microarray analysis, selective COX-2 inhibitor was distinguished by its gene expression profiles amongst different anti-inflammatory drugs. Understanding inflammatory cascades initiated by SCI should allow design of improved therapies.

Key Words: DNA Microarrays, Clustering Analysis, Cycloxygenase-2, Gene Expression

DRAFT

Introduction

Initial mechanical disruption of spinal cord tissue leads to destruction of cells at the injury site. The injury activates enzymatic mechanisms and initiates inflammatory responses. Typically, the cell membrane is damaged and phospholipase A_2 (PLA_2) can be activated to hydrolyze membrane phospholipids into arachidonic acid and this leads to production of eicosanoids. Inflammatory mediators (e.g. nitric oxide, prostaglandins, cytokines) are quickly released. Peripheral cells (e.g. monocytes, neutrophils and lymphocytes) start to infiltrate and accumulate at injury site as early as one day after injury. Increased vascular permeability and loss of cellular fluid leads to tissue edema and results in ischemia. Subsequently, neuron and glial cells undergo necrotic and apoptotic cell death. These events exacerbate secondary cell death and result in ultimately permanent tissue damage and a loss of motor function. A potent anti-inflammatory treatment, methylprednisolone (MP) has been show to rescue 20% of motor function in human clinical trials, and this effect is thought to be associated with its strong inhibition of lipid peroxidation and inflammatory cytokine production (Xu et al., 1998;).

In the clinic, chronic pain syndrome is also a severe complication in patients chronically paralyzed (Beric et al., 1998; Davidoff et al., 1991), and this pain has been shown to be related to production of PGs (Hains et al., 2001). With the utmost relevance, the cyclooxygenase pathway mediates the formation of eicosanoids, including PGs.

Cyclooxygenase (COX; prostaglandin H2 synthetase) is a key enzyme for hydrolysis of arachidonic acid. There are two gene isoforms of cyclooxygenase in mammals, COX-1 and COX-2. Both are membrane-bound enzymes with a 71 kDa molecular weight and 63% amino acid sequence homology (Vane et al., 1998). There is a long narrow channel with a side pocket in the enzyme structure, which can contain and catalyze arachidonic acid (Wong et al., 1997). Even though the two forms of cyclooxygenase (COX-1 and COX-2) share similar activity, they differ in their expression and distribution.

In periphery, COX-1 is constitutively expressed and responsible for physiological production of PGs in tissues such as stomach and kidney, whereas COX-2 is the inducible form that accounts for the pathological production of PGs in different conditions, such as inflammation and cancer (Vane et al., 1998). Induced COX-2 gene expression, protein levels and enhanced eicosanoids have been shown to induce pathological progress in SCI (Resnick et al., 1998; Hains et al., 2001). Arachidonic acid (AA), which is the major precursor of PGs, is cleaved from cell membrane phospholipids by the action of phospholipase A_2 (PLA_2) and phospholipase C (PLC). AA is in turn transformed into PGs, the ubiquitous fatty-acid derivatives, by the action of COX enzyme isoforms. It has been shown that PGs can act synergistically with IL-1. Initial release of PGs from AA by COX-1 (constitutive form) contributes to IL-1's bioavailability to stimulate COX-2 (inducible form) synthesis for more PGs. PGs are responsible for most of the IL-1-induced effects such as typical inflammation symptoms (fever, pain) (4).

DRAFT

Further enzymatic conversion of PGH_2 into other PGs and thromboxane, is exerted by prostacyclin synthase and various isomerases. Lipoxygenase (5- and 12-) can also act on AA and produce HPETE derivatives (Cook et al., 1993).

The COX-2 gene is a small (8.3 kb) immediate early gene, while COX-1 is a much larger (22 kb) gene (Vane et al., 1998). In the CNS, COX-1 mRNA is detectable in dorsal root ganglion (DRG) (Inoue et al., 1999). "Basal" level of COX-2 mRNA and protein are detectable in neurons of forebrain (Breder et al., 1995; Cao et al., 1995). COX-2 mRNA is increased by LPS and IL-1 stimulation of brain tissue and cultured glial cells (Breder et al., 1995; Cao et al., 1996). COX-1 and COX-2 mRNA (Hay and de Belleroche, 1998; Guhring et al., 2000) and protein (Resnick et al., 1998; Ebersberger et al., 1999) are also found in spinal cord. Typically, COX-1 is expressed in many tissues, including gastrointestinal tract and kidney. As an inducible immediate early gene, COX-2 is expressed primarily in brain and macrophages. (Kujubu and Herschman, 1992; O'Banion et al., 1992; Feng et al., 1993). In CNS, COX-1 and COX-2 are found in both neuron and non-neuronal cells in CNS (Strauss et al., 2000). In CNS, COX-1 is thought to be responsible for housekeeping actions of PGs, while COX-2 is induced by various conditions, such as cytokines, growth factors, traumatic injury and acute and chronic inflammation. After spinal injury, pathological tissue damage and oxidative stress activate expression of COX-2, which plays a potential role in hypoxia-induced or excitatory amino acid (EAA)-induced neuronal cell death (Strauss and Marini, 2002).

COX-2 inhibitors are novel anti-inflammatory and analgesic agents that selectively inhibit COX-2 over COX-1, with three orders of magnitude greater affinities. This avoids the disadvantage of gastrointestinal side effect by non-selective COX inhibition. Specific inhibition of COX-2 by NS398 can preserve neuronal function after hypoxia/ischemia in piglet (Domoki et al., 2001). SC58125, a highly selective COX-2 inhibitor, has shown significant ability to improve functional outcome after experimental spinal contusion (Resnick et al., 1998). Currently, the widely accepted mechanism of COX-2 inhibitor in reducing pathological damage and behavioral deficits is its effectiveness of suppressing the COX-mediated PG synthesis (Hains et al., 2001). In addition to inhibiting COX, the result is not only a decrease in PG synthesis, but low production of other prostanoids (e.g. thromboxanes) as well. More arachidonic acids are then made available for synthesis of other compounds in lipoxygenase pathway and endocannabinoid production (Panikashvili et al., 2001; Strauss et al., 2002). COX-2 inhibition may also rescue neuronal survival through the ERK pathway, which is independent of the COX pathway (Vartiainen et al., 2001). The consequences of COX inhibition in these processes have not been systematically studied in the CNS.

In SCI, since the status of cells alters, mRNAs associated with the injury state will be affected. A detailed and global knowledge of subsequent gene expression changes following injury or treatment could provide meaningful insight of molecular mechanisms in SCI that could be reasonable targets for therapeutic intervention. In the present study, we applied DNA microarrays to compare gene expression following the five anti-

DRAFT

inflammatory treatments. We expected to see a major similarity between these treatments due to their anti-inflammatory mechanisms. However, it was hypothesized in this work that there may also be some novel molecular mechanisms of one compound over others. Four hours following slice culture (a model of tissue injury), expression of 5,000 genes was measured by our custom rat microarrays. A number of statistical analyses (i.e. principal components analysis [PCA], gene shaving; K-medians/Relative Data Depth [ReD]) were applied to the data. A unique pattern of gene expression was revealed, in which a cluster of genes were only up-regulated by the COX-2 inhibitor. Functions of those genes could be associated with beneficial immune activities, initiation of regenerative capacity, protective stress responses etc. COX-2 inhibitor distinguished itself by its target on the above gene expression profile, which can be predicted as an overall beneficial effect in reducing tissue damage after spinal cord injury. In summary, microarray analysis revealed a unique pattern of gene expression by COX-2 inhibition, which was indicated as neuroprotection against tissue damage after acute spinal cord injury in vivo.

DRAFT

Materials and Methods

Animal Injury Cultured spinal cord slices were used as a model of SCI (Pan et al., 2002). Adult rat spinal cords were quickly isolated, and then 1 mm slices were placed in wells of a 24-well tissue culture plate. Four slices were typically placed in a single well with 0.5 ml of Opti-MEM medium with 1% N2 supplement (Life Technologies). The cultures were incubated at 37°C and 5% CO_2 for up to 4 hrs, and then frozen for RNA analysis. In the experiments, groups of cultures were treated with each of 5 anti-inflammatory compounds: [1] acetaminophen (pretreatment 100 mg/kg i.p.; 2 mM in culture); [2] indomethacin (pretreatment 10 mg/kg i.p.; 10 mM culture); [3] MP (pretreatment 30 mg/kg i.p.; 0.5 mg/kg culture); [4] NS398 (pretreatment 5 mg/kg i.p.; 100nM culture); and [5] a mixture of 500 ng/ml rat recombinant IL-1 receptor antagonist and 3.2 mg/ml soluble TNF receptor:Fc chimeric protein. In most cases, animals were pretreated with drug 1 hr prior to explantation. Each group consisted of 3 independent cultures analyzed independently. Control groups included both freshly-dissected spinal tissue (uninjured), and vehicle-treated cultures. Total cellular RNA was prepared and analyzed using microarrays.

Long-Evans rats were pretreated with NS398 (10 mg/kg i.p.) or vehicle intraperitoneally 1 hour before surgery. After deep anesthesia, rats were applied thoracic (T9-T10) laminectomy. A 10 g × 2.0 mm diameter rod was released from a 25-mm height onto the exposed spinal cord, using NYU impactor injury model. Immediately after contusion, rats were treated with another dose (10 mg/kg i.p.). Twelve hours following

DRAFT

injury, the rats were euthanized and spinal tissue was isolated for further atomic absorption spectroscopy and mRNAs analysis

Atomic absorption spectroscopy. Tissues were weighed to obtain the wet weight before homogenization in Trizol (Invitrogen) to extract RNA. An aliquot (50 µl) of the Trizol homogenate was removed and diluted in distilled water for atomic absorption spectroscopy to measure potassium using a Perkin-Elmer 3100 spectrometer. Trizol alone contains no detectable K^+ (not shown). Results were expressed as µmol K per g of tissue.

Microarrays The 4,967 probes on our custom microarrays contains a collection of 4,854 oligonucleotides specific for 4,803 rat cDNA clusters purchased from Compugen, Inc. (Jamesburg NJ) and a set of 113 oligos designed and synthesized by MWG-Biotech AG (Ebersberg, Germany) based on a set of GenBank accession numbers provided by us. The probes, 65-70nt in length, are standardized for melting temperature and homology is minimized. All bioinformatics for the oligonucleotides are provided on our searchable web site, www.ngelab.org. Microarrays were printed on poly-L-lysine-coated glass slides using an OmniGrid microarrayer (GeneMachines, San Carlos CA) and quill-type printing pins. Poly-L-lysine slides were prepared and scanned at 532nm and 635nm in a GenePix 4000A Scanner (Axon Instruments Inc., Union City CA) to evaluate surface quality. Slides were stored in a bench-top desiccator for at least three weeks prior to use.

Oligonucleotides were resuspended to 40 µM in 3X SSC and rehydrated with shaking at room temperature. Printing was performed at 24°C with a relative humidity of approximately 50%. After printing, arrays were stored overnight in a parafilm-sealed plastic slide box in a desiccator at room temperature and post-processed by standard procedures. Slides were stored at room temperature in a sealed plastic slide box in a desiccator and used for up to three months after printing.

Hybridization. RNA was prepared from drug or vehicle treated sliced cultures. Tissues were homogenized with a tissue grinder. Chloroform was added to the Trizol homogenate. A volume of 0.25 ml of aqueous phase following chloroform extraction of the Trizol homogenate was mixed with an equal volume of 70% ethanol and loaded onto an RNeasy column (Qiagen, Valencia CA). The column was washed and RNA eluted following the manufacturer's recommendations. RNA was subjected to spectroscopic analysis of quantity and purity, with A_{260}/A_{280} ratios between 1.9 and 2.1 for all samples. All samples of injured cord RNA and vehicle controls were subjected to gel electrophoresis on an Agilent (Palo Alto CA) 2100 Bioanalyzer; all samples demonstrated both sharp 18S and 28S ribosomal RNA bands. Sample of total cellular RNA were used for both microarrays and Q-RT-PCR

Fluorescent probes were prepared using the Genisphere 3DNA dendrimer system (Genisphere, Inc., Montvale NJ). Two micrograms of total cellular RNA were reverse-transcribed from a "capture-sequence"-containing oligo-$d(T)_{18}$ primer using Superscript II (Invitrogen). Following alkaline hydrolysis and ethanol precipitation, the cDNA was pre-hybridized with dye- and capture sequence-specific fluorescent dendrimers at 53°C

DRAFT

for 45 min. Tagged probes were then hybridized with microarrays in hybridization buffer (0.25 M $NaPO_4$, 4.5% SDS, 1 mM EDTA, 1X SSC, 1 μg of rat Cot-1 DNA [Rat Hybloc, Applied Genetics Laboratories, Melbourne FL], and 2 μl of Capture Blocker [Genisphere]) using a GeneMachines hybridization chamber. The following day the arrays were washed and scanned on an Axon GenePix 4000B.

Data Analysis Image files were processed using Axon GenePix 4.0 software, resulting in text files containing median fluorescence intensities as well as median local backgrounds. GenePix flagged spots near background as unreliable, and we manually flagged spots with unusual problems. The text files were loaded into an open-source, MIAME-compliant, web accessible database (BASE; Saal et al. 2002). Data were then imported into GeneSpring (Silicon Genetics, Redwood City CA). We used the "Per chip, Per spot Lowess" method of normalization provided in GeneSpring. Normalized data were filtered by ANOVA at $p<0.05$ using the Benjamini and Hochberg False Discovery Rate for multiple measurement corrections. Principal Components Analysis (PCA), Gene Shaving, K-Median and Relative Data Depth run independently (details in each figure).

Quantitative Real-time PCR We confirmed selected microarray results by comparison with mRNA levels obtained by quantitative reverse transcription PCR (Q-RT-PCR) using selected gene-specific primer pairs. RNA was reverse transcribed with SuperScript II and random primers as suggested by the manufacturer (Invitrogen). The PCR reactions were carried out using 10 ng of cDNA, 50 nM of each primer, and SYBR Green master mix (Applied Biosystems, Foster City CA) in 10 μl reactions. Levels of Q-RT-PCR product were measured using SYBR Green fluorescence (Wittwer et al., 1997; Ririe et al., 1997) collected during real-time PCR on an Applied Biosystems 7900HT system. A control cDNA dilution series was created for each gene to establish a standard curve. Each reaction was subjected to melting point analysis to confirm single amplified products.

DRAFT
DRAFT

Results

Inflammatory responses are notorious for exacerbating secondary tissue damage following spinal cord injury. Anti-inflammatory treatments have been shown to be effective to reduce inflammation and spare spinal tissue for functional improvement. Previously we have detected a localized inflammatory cytokine response after acute spinal cord contusion. Using slice cultures (Pan et al., 2002), we found that this cytokine mRNA induction does not require infiltrating peripheral cells and was a result of pre-existing cytokine activation. Applying cytokine receptor blockers or using mice with knocked-out cytokine receptors, cytokine mRNA accumulation was significantly diminished (Pan et al, 2002). This injury model allows us to concentrate on the gene expression change in spinal tissue itself early after injury. Therefore, pattern of gene responses in our assay would help to predict subsequent biological events in secondary injury.

In the current work, adult rat spinal cords were freshly removed and sliced into 1 mm segments (which served as the "injury" to spinal cord). In order to identify anti-inflammatory reagents that produced a novel gene response in injured spinal cord tissue, groups of spinal cord cultures were treated with each of 5 anti-inflammatory compounds: acetaminophen, indomethacin, MP, NS398 and a mixture of rat recombinant IL-1 receptor antagonist and soluble TNF receptor:Fc. In most cases, rats were pretreated with drugs to achieve maximal effect at the time of injury. Since all compounds were anti-inflammatory, it was expected that there would be a large extent of overlapping gene response. However, we would like to see the differences in mRNA effect by these treatments and identify novel mechanisms beyond anti-inflammation.

Spotted glass microarrays with 4,916 genes were prepared on poly-l-lysine coated glass slides. Each array was hybridized with fluorescence labeled cDNAs specific for treatment group and control sample. Data were normalized using Lowess and loaded into public database, http://base.rutgers.edu. In Figure 1, the dataset was filtered by ANOVA at $p<0.05$ using the Benjamini and Hochberg False Discovery Rate for multiple measurements corrections, which produced a subgroup of 314 genes that were significantly altered in any condition. We concluded that this group of genes could serve as a proxy for the effects of each compound on spinal tissue in the presence of injury.

This subset was then log-transformed, centered, and the eigenvectors constituting the principal components of the set were calculated (Figure 2). The goal of using principal components analysis (PCA) was to identify major gene regulatory patterns in the dataset and to ascribe the proportion of total variability explained by each eigenvector. This allows us to focus only on those eigenvectors corresponding to 10% or more of the variability. The first eigenvector, which explained nearly 50% of the total variability, included similar values for each of the 5 anti-inflammatory treatments. This was expected, but uninteresting. The second eigenvector, explaining approximately 25% of the variability, described a surprising effect within our experiment. This vector described a pattern of response that was quite unique to NS398, the COX-2 inhibitor. We interpreted this result as demonstrating a unique pattern of cellular mechanisms affected

DRAFT

by COX-2 inhibition during spinal cord injury. These unique mechanisms represented the goal of our analysis. However, since PCA does not partition the data, we were unable to interpret the response pattern biologically.

Genes were clustered by "gene shaving" (Figure 3) those genes orthogonal to the principal components. The group corresponding to the second principal component and included only 11 genes, ranging from chemokines (MCP-1, MIP-1α) to stress responses (Hsp 70, heme oxygenase) to those with somewhat unknown function (decorin, T-cell death associated gene). The identities of genes within this cluster were interpreted as potentially protective to injured tissue.

In a separate approach, the 314 gene ANOVA-selected genes were clustered by K-medians (Figure 4). We find that K-medians clustering produces more robust clusters than the more commonly-used K-means method. Resulting clusters were examined for fit within their assigned clusters using the newly-described Relative Data Depth (ReD; Jörnsten, manuscript in press) method (Fig. 5). ReD compares unit vector fit or each gene within each cluster with fit to adjacent clusters. Combining these two methods, we find one K-Medians cluster with excellent fit by ReD that also roughly corresponds to the pattern of the second principal component. This cluster was also uniquely up-regulated by NS398. This cluster contains only 7 genes and is a subset of the gene shaving cluster. The combination of these two clustering methods (Figure 7) allows us to focus on the most reproducible, most robust effects that are specific for NS398. Selected genes from microarray result were confirmed in their changes between drug treated and vehicle controls (Figure 8). Again, our interpretation of the genes within this cluster suggests a protective function following SCI.

To test our hypothesis, we performed an in vivo contusion injury and we assessed the lesion volume after NS398 treatment. NS398 treatment resulted in a significant reduction in lesion area and a spreading neuroprotective effect on injury site and adjacent segments (Figure 9).

DRAFT
DRAFT

Discussion

Examination of the putative roles of these selective genes suggests that NS398 may promote attraction of activated macrophages (MCP-1; MIP-1α), which we interpret as beneficial for removal of cellular debris from the injury site, assuming that an appropriate activation signal is present. Stress responses, such as heme oxygenase and possibly, Hsp 70, have been shown to be protective, particularly when induced prior to injury. Placental lactogen, a member of the prolactin hormone gene family, is associated with angiogenesis and blood vessel remodeling, including endothelial cell proliferation, migration, protease production and apoptosis. Vimentin, in this context, is likely a sign of astrocytic or ependymal cell remodeling. Some studies identify vimentin staining as a phenotype potentially conducive for regenerative capacity, although this is not yet proven. Matrix Gla protein is known to be involved in vascular calcification, but also can be induced by bFGF, retinoic acid, estrogen, and TGFβ in chondrocytes, lung, and kidney. Matrix Gla has also been shown to induce expression of BMP-2, a powerful regulator of neuronal development and phenotype. Finally, decorin, a member of the small praline-rich proteoglycans, modulates collagen fibrillogenesis, inhibits proliferation and protects macrophages from the induction of apoptosis, and reverses the TGFβ-mediated repression of macrophage activation. Interestingly, while reduction of decorin levels promotes scar-less healing of peripheral injuries, ectopic addition of decorin protein reduced CNS glial scarring following cortical incision. This list of genes and their potential effects provides rich fodder for generating testable hypothesis of mechanisms mediating COX-2 antagonist function. However, we interpret this list of genes as being overall beneficial for tissue resolution, protection from stress responses, blood vessel remodeling, astrocytic remodeling, neuronal differentiation, macrophage activation, and reduced glial scarring. We are also aware of the possible shunting of arachidonates into endocannabinoids, which themselves may be neuroprotective.

DRAFT
DRAFT

Figure legends

Figure 1 DNA microarray analysis of five different anti-inflammatory treatments after spinal cord injury. The data was collected from 4 hr cultures with five different treatments (methylprednisolone, acetaminophen, indomethacin, NS398, and cytokine inhibitors) compared to vehicle treated. Individual uninjured and injured versus pooled uninjured samples (all with no treatment) were included as control conditions. The expression ratio represents fold change of the genes after drug treatments in individual culture samples. Pooled vehicle control was used to eliminate the between-sample variation in individual uninjured and 4 hr injured samples. Part A showed expression ratio of 4,803 genes at seven conditions. Using statistical filtering analysis, (ANOVA $p<0.05$, Benjamini and Hochberg's False Discovery Rate, B&H FDR), 314 genes passed the restriction and were retained for further analysis (Part B).

Figure 2 Principal Components Analysis (data matrix centered) revealed unexpected gene expression by COX-2 inhibitor. In principal components analysis (Part A), six principal components were identified with the corresponding eigenvalues. Each principal component represented a particular gene expression pattern. In Part B, scree plot shows percentage of the total variances explained by each principal component. In the graph, principal components were sorted by their accounted variances. In the analysis, components after where the curve leveled off were discarded due to insignificance of explained variance and uninformative. Specifically, eigenvector 1 (red color) was shown to account 50% of overall variance, which is significantly large, but not interesting since the gene expression pattern is similar across treatments. Eigenvector 2 (green color), which accounts for 25% of the total variance revealed an unexpected expression profile, in which genes were only up-regulated by COX-2 inhibitor, NS398.

Figure 3 PC based Gene Shaving Accentuated Unique Pattern By COX-2 Inhibition Gene Shaving (based on principal components) formulated each principal components, starting with the first principal component. The algorithm shaved the most uncorrelated genes off, and repeated the shaving procedure until finally there is only one gene left. Then all the genes were sorted by their correlation to each principal component. Appropriate cluster size was determined thereafter, in which genes contributed to the each cluster equally. Not surprisingly, clusters identified by gene shaving correlated well with the components by PCA. Moreover, it accentuated the significance of the first (red color) and second clusters (green color) in the corresponding explained variance. The second cluster was again identified as a unique pattern by COX-2 inhibitor.

Figure 4 Distinct profile by COX-2 inhibition in Gene Shaving (heat map). In the heat map result of gene shaving, seven treatments were shown on the X-axis. Six clusters of gene identified were listed from bottom to the top on Y-axis. "Red" color represented down-regulation of the genes, and "Yellow" as up-regulation. Genes were expressed equally in both conditions in "Orange". Clearly, in cluster one, gene expression ratios

DRAFT

were similar in different drug treatments. Amongst the seven conditions in the second clusters, COX-2 inhibitor uniformly up-regulated the genes.

Figure 5 K-Medians distinguishes COX-2 inhibitor from other treatments. In K-Median clustering, five centroids were selected as the centers of gene clusters. Distance from each observation (gene) to the centroids was calculated and genes were grouped to the closest center. In Part A, five clusters were identified with different profiles. The fifth cluster stood out uniquely with significant up-regulation by COX-2 inhibitor. In Part B, the genes included in the cluster were uniformly grouped together, whose function will be discussed in the following paragraphs.

Figure 6 Relative Data Depth validated and improved accuracy of K-medians clustering. We further performed relative data depth (ReD), recently described by Rebecka Jörnsten) to confirm the results from K-Median and validate the clusters. ReD calculates the relative data depth from each observation (gene) to centers of the data matrix, which are shown as the bars on the top part of the graph. Instead of measuring distance, it allows to measure vector pointing from genes to the cluster centers, which makes this method independent of data scale. The protrusions at the bottom part of the graph represent the noise (outliers) inside the each cluster. Five clusters were presented along the X-axis from the left to the right. Apparently, the cluster at the far right end of the graph has very few outliers and presented as a well-isolated cluster of genes. This result confirmed the clusters from K-Medians and improved the accuracy of the gene list inside it.

Figure 7 Identification of the most reproducible gene list only up-regulated by COX-2 inhibitor using multiple statistical analyses. In this table, genes identified by different methods were listed on the Y-axis. Black box checked the presence of the genes in particular analysis. It is quite obvious that several statistical methods (PCA, Gene Shaving, and K-Medians/ReD) shared quite number of genes in common, while some difference was still noted. In conclusion, by combining multiple different statistical analysis would allow us to focus on the most reproducible list of genes and the most robust effect specific to COX-2 inhibitor. Amongst the genes in common, monocyte chemoattractant protein-1 (MCP-1) has been shown to promote attraction of activated macrophages, which can be explained as beneficial removal of cellular debris from the injury site. Decorin, a gene that can relieve CNS injury scar formation, has been indicated to reverse the suppression of macrophage by TGF. Placental lactogen-1, a family member of prolactin hormone, is associated to angiogenesis and blood vessel remodeling. Vimentin has been shown to be conducive to neurogenesis. Finally, heat shock protein (hsp)-70 and heme oxygenase-1 have both been implicated to induce protective stress response in ischemia injury model. Therefore, the overall effect by up-regulating these genes would be predicted as protective and pro-repair.

DRAFT

Figure 8 Confirmation of mRNA changes by Quantitative Real-time PCR

Quantitative Real-time PCR are conducted to verify the changes of the genes observed in microarray analysis. GAPDH is used as internal control to correct the difference in mRNA amount for each sample. Gene expressions were shown by log ratio of drug treated vs vehicle control. As shown in Figure 8, Q-RT-PCR shows good agreement with microarray data in regulation pattern for the corresponding genes. The magnitude of gene regulation is found more prominent in Q-RT-PCR than in microarray analysis. In general, the two separate approaches confirm the same effect of NS398 revealed by statistical analysis.

Figure 9 Selective COX-2 inhibitor significantly reduce lesion after acute SCI. One hour prior to injury, rats were treated with NS398 or vehicle. Upon contusion injury, rats were raised for 6 hr and sacrificed for atomic absorption measurement. It showed that there was significant reduction of lesion volume in NS398 (selective cyclooxygenase-2 inhibitor) treated animals. Furthermore, this protective effect from NS398 extends both rostrally and caudally.

DRAFT

Figures

Figure 1 Statistical filtering by ANOVA

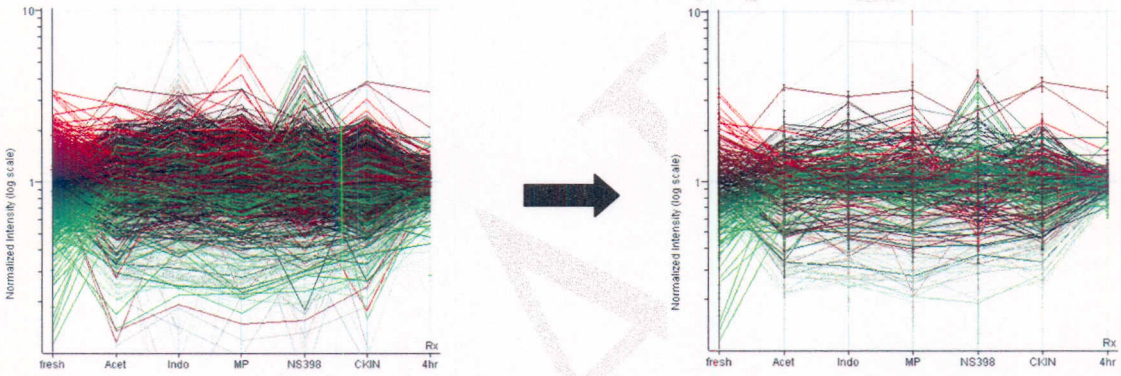

DRAFT

Figure 2 Centered - PCA

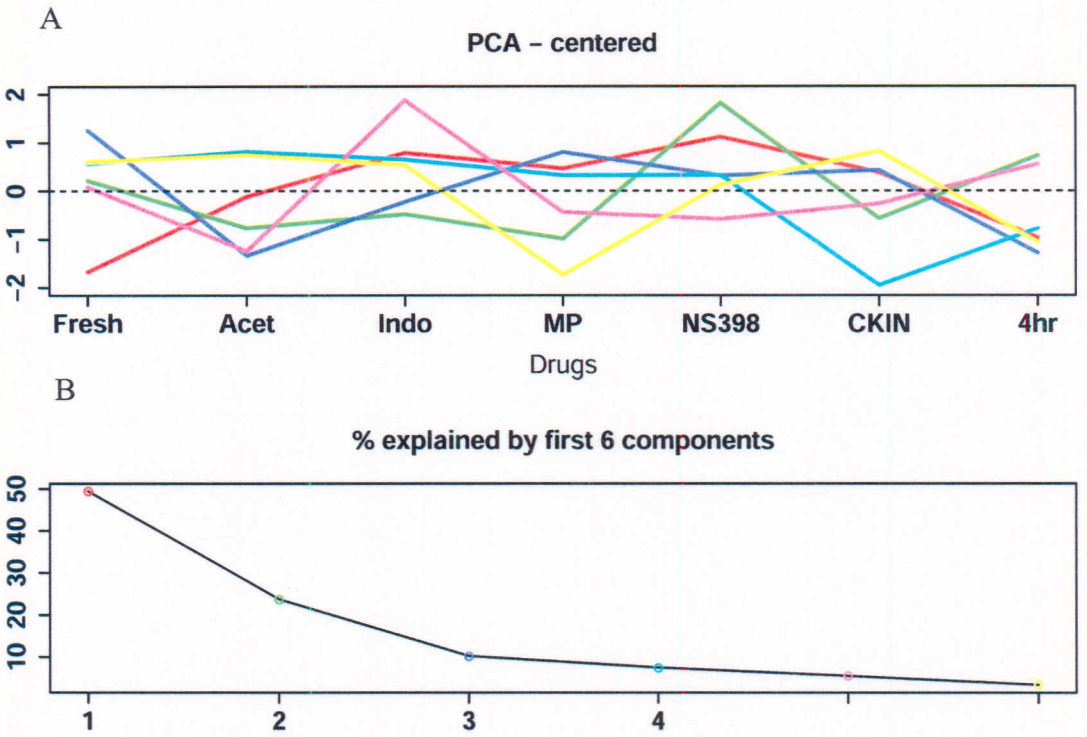

Figure 3 Gene Shaving

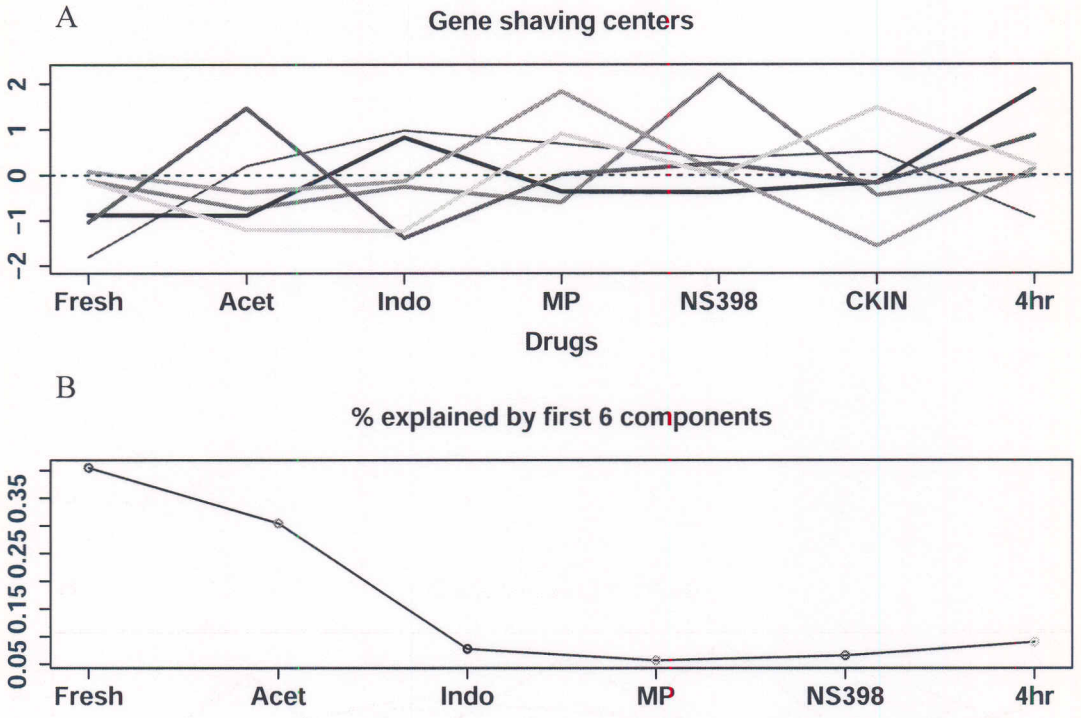

Figure 4 Heat-map representation of Gene Shaving

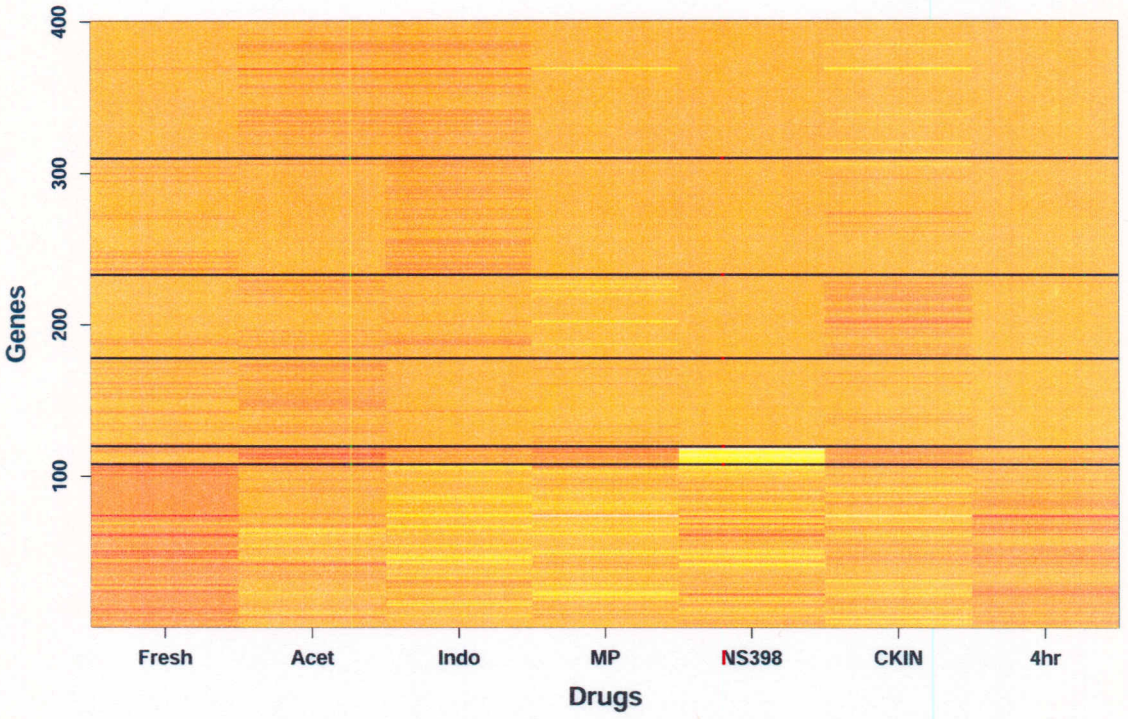

Figure 5 K-Median Clusters

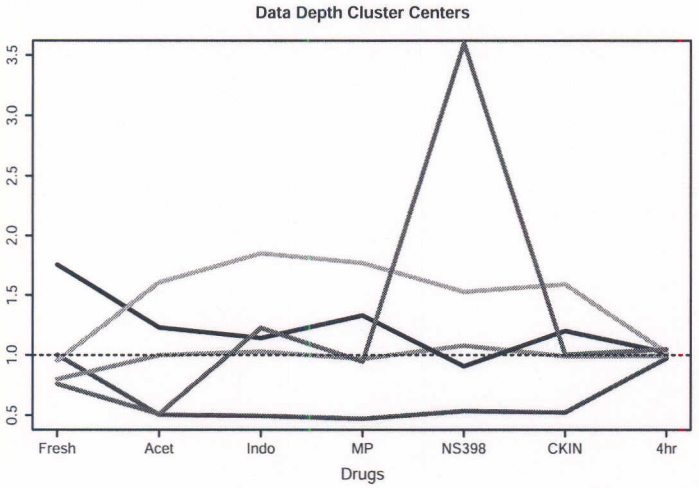

DRAFT

Figure 6 Relative Data Depth (ReD)

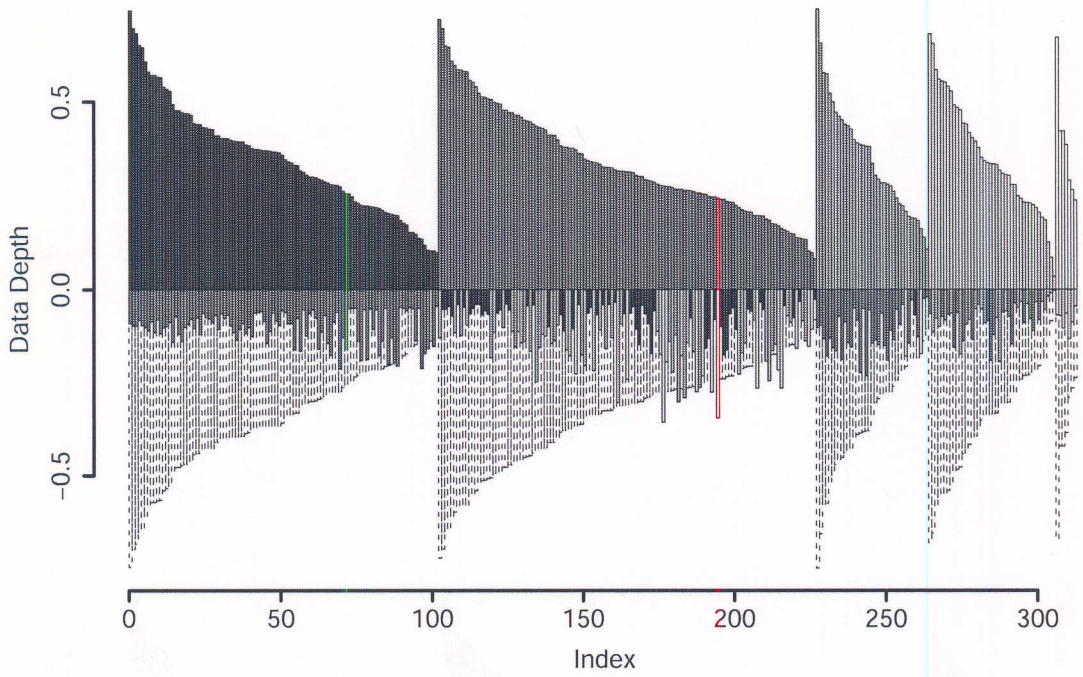

Figure 7 Comparison of multiple statistical analyses

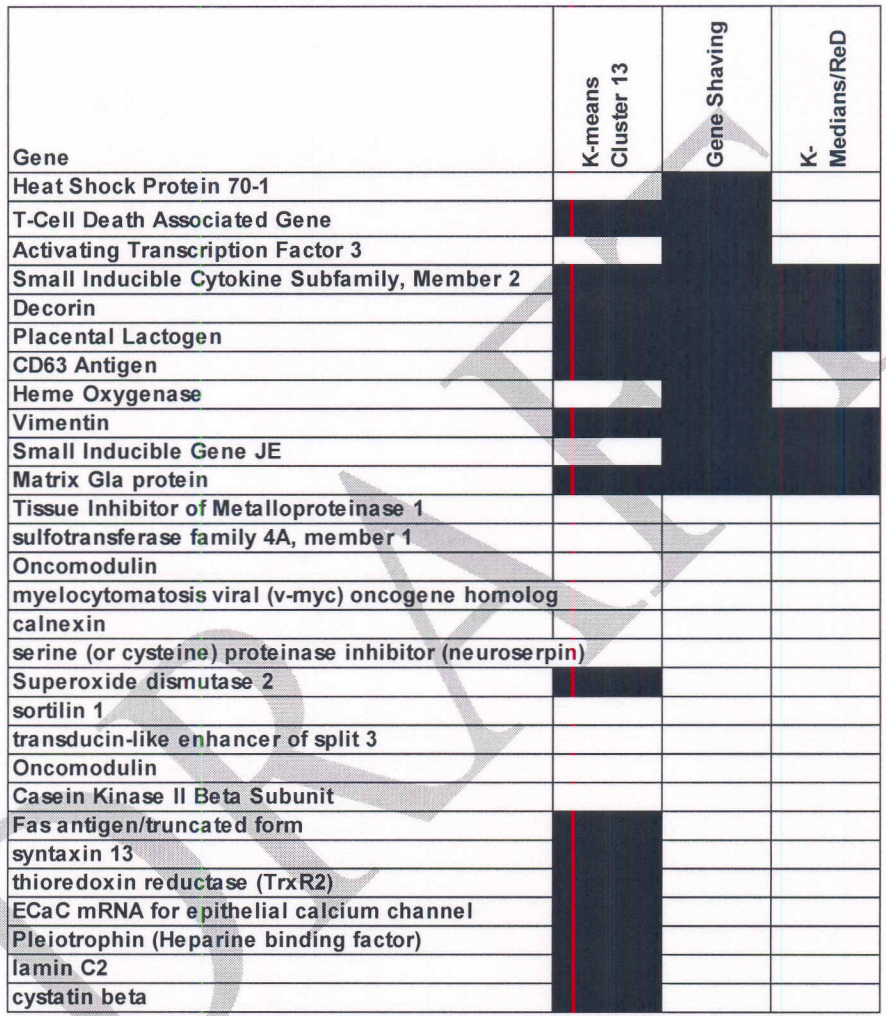

Figure 8 Confirmation of mRNA change by Quantitative Real-time PCR

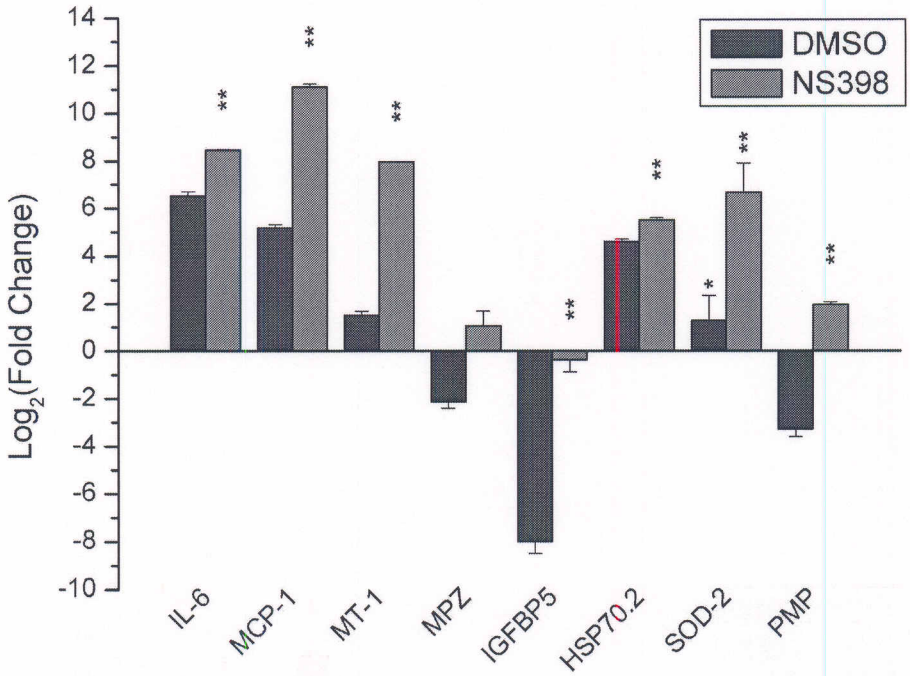

Figure 9 Lesion Volume Reduction by COX-2 inhibitor

Part A

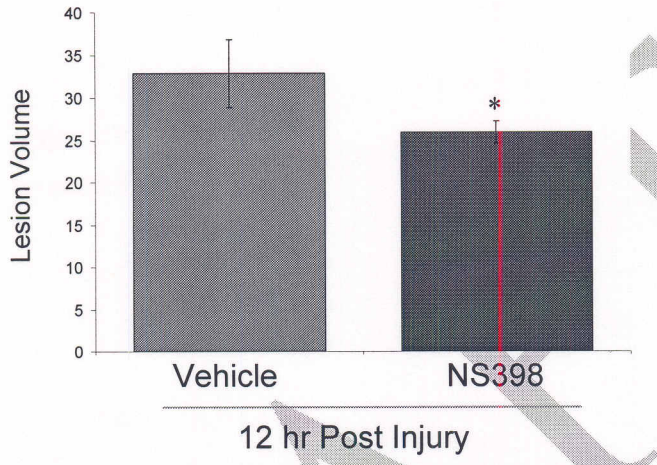

* p<0.05 by ANOVA with Bonferroni post-hoc

Part B